

University of Texas Rio Grande Valley

ScholarWorks @ UTRGV

Mechanical Engineering Faculty Publications
and Presentations

College of Engineering and Computer Science

10-1-2021

Numerical Study of Fully Coupled Fluid-Structure Interaction of Stented Ureter by Varying the Stent Side-Holes

Erick Martinez

The University of Texas Rio Grande Valley

Ben Xu

Jianzhi Li

The University of Texas Rio Grande Valley

Yingchen Yang

The University of Texas Rio Grande Valley, yingchen.yang@utrgv.edu

Follow this and additional works at: https://scholarworks.utrgv.edu/me_fac



Part of the [Biomechanical Engineering Commons](#), and the [Medicine and Health Sciences Commons](#)

Recommended Citation

Martinez, E, Xu, B, Li, J, & Yang, Y. "Numerical Study of Fully Coupled Fluid-Structure Interaction of Stented Ureter by Varying the Stent Side-Holes." Proceedings of the ASME 2021 Fluids Engineering Division Summer Meeting. Volume 1: Aerospace Engineering Division Joint Track; Computational Fluid Dynamics. Virtual, Online. August 10–12, 2021. V001T02A037. ASME. <https://doi.org/10.1115/FEDSM2021-64044>

This Conference Proceeding is brought to you for free and open access by the College of Engineering and Computer Science at ScholarWorks @ UTRGV. It has been accepted for inclusion in Mechanical Engineering Faculty Publications and Presentations by an authorized administrator of ScholarWorks @ UTRGV. For more information, please contact justin.white@utrgv.edu, william.flores01@utrgv.edu.

NUMERICAL STUDY OF FULLY COUPLED FLUID-STRUCTURE INTERACTION OF STENTED URETER BY VARYING THE STENT SIDE-HOLES

Erick Martinez

Depart. of Mechanical Engineering, The University of Texas Rio Grande Valley, Edinburg, TX 78539

Ben Xu*

Depart. of Mechanical Engineering, Mississippi State University, Mississippi State, MS 39762
xu@me.msstate.edu

Jianzhi Li

Depart. of Manufacturing and Industrial Engineering, The University of Texas Rio Grande Valley, Edinburg, TX 78539

Yingchen Yang

Depart. of Mechanical Engineering, The University of Texas Rio Grande Valley, Edinburg, TX 78539

ABSTRACT

Ureteral stents are a measure used for many medical issues involving urology, such as kidney stones or kidney transplants. The purpose of applying stents is to help relieve the urine flow while the ureter is either blocked or trying to close itself, which creates blockages. These ureteral stents, while necessary, cause pain and discomfort to patients due to them being a solid that moves around inside the patients' body. The ureter normally moves urine to the bladder through peristaltic forces. Due to the ureter being a hyperelastic material, these peristaltic forces cause the ureter to deform easily, making it necessary for the stent to properly move the urine that flows through it for the patient not to face further medical complications. In this study, we seek to find a relation between the amount of stent side holes and the overall flow rate inside the stent with the ureter contracting due to peristalsis. A fully coupled fluid-structure interaction (FSI) model is developed to visualize how the ureter deforms due to peristalsis and the subsequent effect on the urine flow due to the ureter's deformation. Numerical simulations using COMSOL Multiphysics, a commercial finite-element based solver, were used to study the fluid-structure interaction, and determine whether the stent performs more properly as the amount of stent side holes increases. The results showed that the stent model with a 10 mm distance between side hole pairs provided the highest outlet flow rate, which indicates a proper stent design that allows for maximized urine discharge. We hope this study can help improve the stent design in kidney transplant procedures to further ease the inconvenience on the patients.

Keywords: Computational Fluid Dynamics (CFD), Multiphysics, Fluid-Structure Interaction (FSI), ureter stent, peristalsis

1. INTRODUCTION

Currently, the plastic and silastic stents used by urologists around the world cause many inconveniences due to the discomfort the patients experience during its time inside the

ureter tract. With the stents being deformable and having free motion within the ureter, the subject will encounter discomfort and pain from the deformation of the stent that translates into a reaction force that the ureter walls must compensate. The insertion of the stent has different motives: kidney transplant procedures, urological failures, kidney stones, etc. The purpose of the stent is to normalize the flow of urine in the ureter, which either tries to close itself following a kidney transplant, or experiences blockages in the case of kidney stones. The stent is followingly removed a few weeks after the healing process and once the urine flow has been completely normalized. An example diagram of what the ureter looks like when installed can be seen in Figure 1.

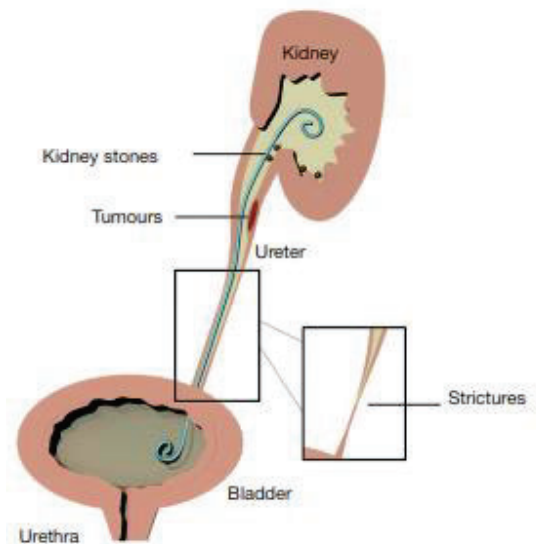


FIGURE 1: Urinary tract with presence of stent [5]

These ureter stents have differing lengths depending on each patient's case and have an annular cross section to allow for urine

to flow through. The stent side holes allow for the urine to enter it and make its way to the bladder. Presently, there has not been a fully coupled fluid-structure interaction study performed in a stented ureter driven by peristalsis, so the study will also provide valuable information regarding the stress during urinary flow.

Numerical simulations from the work of Takaddus [14-17] have changed the peristaltic force driving the urine flow from being a contracting force to an expansive one [14]. The expanding of the ureter develops a bolus of urine that flows down, however, it also develops a backflow towards the renal pelvis due to the high pressure created around the area of expansion.

Additionally, to the fluid dynamics simulation, we are also interested in how the fluid flow will deform the ureter walls and inserted stent. Because of this, a fluid-structure interaction (FSI) simulation must be performed where the deformation of the ureter drives the flow and subsequently, causes loadings on the stent itself. This study adopted COMSOL Multiphysics due to its potential to combine physics such as fluid dynamics and solid mechanics. The purpose of this study is to numerically explore the laminar flow profile inside the ureter to verify the stent's design. Considering the deformable behavior of the stent and the ureter walls, a two-way FSI simulation was performed to study how the elastic materials will deform and how that deformation will affect the flow, making the fluid and elastic deformation simulations fully coupled. Three stent models with side holes along their length were studied to confirm the relationship between wall reaction forces, flow rate and number of holes along the stent. It is hoped that this study will present clear results that can help increase the interest in improving the stents in kidney transplant procedures, as well as optimizing the stents' design to further ease the inconvenience on the patients that require a ureteral stent.

2. MATERIALS AND METHODS

2.1 Computational domain

The numerical model consists in a section of a ureter with a total length of 50 mm and 10 mm total diameter. The ureter wall thickness is 1 mm. [14] The ureteral stent is positioned at the center with an inner diameter of 1 mm and wall thickness of 0.5 mm. The stent side holes have a diameter of 0.5 mm. The urinary bladder and kidney are originally a part of the model, as well as an upper and lower entry for the ureter based on the double J stents. However, since we were more concerned about the results inside the ureter tract itself, they were neglected for this study, as well as to save computational time. The ureter length being 50 mm is also a simplification to shorten simulation time, compared to the real ureteral length of ~30 cm. Three different stent models were created with the changing parameter being the amount of side holes across their length. The models studied have a distance of 25 mm, 10 mm and 5 mm between each side hole pair. Another model without a stent was also used. The dimensional parameters for each stent model used in this study can be found in Table 1.

Model	Distance between side hole pairs	Total amount of side holes
1	0 mm (No Stent)	0 holes
2	5 mm	22 holes
3	10 mm	12 holes
4	25 mm	6 holes

TABLE 1: Model dimensional parameters used in the study

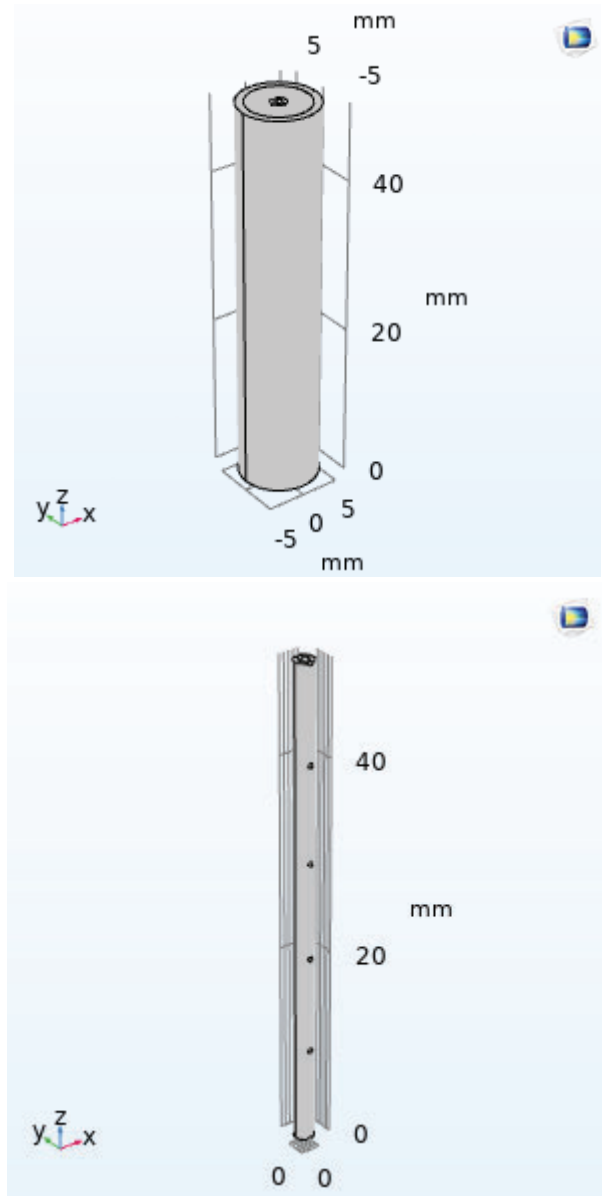


FIGURE 2: Computational domain and example model of stent (10 mm distance between side holes)

2.2 Governing Equations

2.2.1 Fluid domain [4]

Urine is defined as an incompressible liquid. The governing equations for incompressible fluid flow are the continuity and momentum of the Navier-Stokes equations.

$$\rho \nabla \cdot \mathbf{u}_{fluid} = 0 \quad (1)$$

$$\rho \frac{\partial \mathbf{u}_{fluid}}{\partial t} + \rho (\mathbf{u}_{fluid} \cdot \nabla) \mathbf{u}_{fluid} = \nabla \cdot [-p\mathbf{I} + \mathbf{K}] + \mathbf{F} \quad (2)$$

$$\mathbf{K} = \mu (\nabla \mathbf{u}_{fluid} + (\nabla \mathbf{u}_{fluid})^T) \quad (3)$$

The forces considered in the momentum equation come from the deformation of the solid domain due to the fluid-solid interaction. Gravity effects are ignored for this study

At the fluid wall, the no-slip boundary condition is applied which is governed by

$$\mathbf{u}_{fluid@wall} = 0 \quad (4)$$

The inlet and outlet of the ureter are defined as open boundaries, which are governed by

$$[-p\mathbf{I} + \mathbf{K}]\mathbf{n} = -f_0\mathbf{n} \quad (5)$$

2.2.2 Solid domain ^[3]

Due to the transient behavior of the fluid domain, the solid domain will also have a transient equation given by

$$\rho \frac{\partial \mathbf{u}_{solid}}{\partial t} = \nabla \cdot (FS)^T + \mathbf{F}_v \quad (6)$$

$$\mathbf{F} = (\mathbf{I} + \nabla \mathbf{u}_{solid}) \quad (7)$$

where \mathbf{F}_v is defined as the body forces. \mathbf{u}_{solid} is the deformation vector of the solid domain, the second Piola-Kirchhoff stress, S , and the deformation gradient, F .

The domains of ureter and stent have different materials, namely hyperelastic and linear elastic, respectively. As such, they are governed by distinct equations accordingly. For the linearly elastic material, the second Piola-Kirchhoff stress can be found by

$$S = S_{ad} + J_i F_{inel}^{-1} (\mathbf{C} : \varepsilon_{el}) F_{inel}^{-T} \quad (8)$$

In the previous equation, \mathbf{C} represents the constitutive fourth order elasticity tensor and ε_{el} is the elastic strain second order tensor. J_i represents the deviatoric stress tensor. S_{ad} represents any additional stresses the solid domain encounters including initial stresses and external.

$$\varepsilon_{el} = \frac{1}{2} (F_{el}^T F_{el} - I) \quad (9)$$

Here, F_{el} and F_{inel} represent the elastic and inelastic deformation tensors, respectively.

$$\varepsilon = \frac{1}{2} [(\nabla \mathbf{u}_{solid})^T + \nabla \mathbf{u}_{solid} + [(\nabla \mathbf{u}_{solid})^T \nabla \mathbf{u}_{solid}] \quad (11)$$

where ε is the Lagrangian strain tensor, with \mathbf{u}_{solid} being the displacement vector of the solid.

$$\mathbf{C} = \mathbf{C}(E, \nu) \quad (12)$$

The elasticity tensor of the inelastic material is dependent on material properties like the Young's Modulus and the Poisson ratio.

$$S = S_{ext} + \frac{\partial W_s}{\partial \varepsilon} \quad (14)$$

For the hyperelastic material, the second Piola-Kirchhoff stress is calculated from W_s , taking the derivative of it with respect to ε , as well as external stresses.

$$\sigma = J^{-1} F S F^T \quad (15)$$

The Cauchy stress tensor is calculated by the Jacobian of the deformation tensor F and the second Piola-Kirchhoff stress.

$$J = \det(F) \quad (16)$$

The Jacobian of the deformation tensor is given by the previous equation.

$$\mathbf{F} = (\mathbf{I} + \nabla \mathbf{u}_{solid}) \quad (17)$$

Eq. (17) shows how the deformation tensor is calculated, which is then used to calculate the Lagrangian strain of the hyperelastic material.

$$\varepsilon = \frac{1}{2} (F^T F - I) \quad (18)$$

Using the isotropic five parameter Mooney-Rivlin material model, the strain energy density function can be defined by

$$W_s = C_{10}(\bar{I}_1 - 3) + C_{01}(\bar{I}_2 - 3) + C_{20}(\bar{I}_1 - 3)^2 + C_{02}(\bar{I}_2 - 3)^2 + C_{11}(\bar{I}_1 - 3)(\bar{I}_2 - 3) + \frac{1}{2} \kappa (J_{el} - 1)^2 \quad (19)$$

At the fixed constraints, the equation can be written as

$$\mathbf{u}_{solid} = 0 \quad (20)$$

Since the peristaltic force is applied as a boundary load over the outer surface of the ureter, it can be defined as

$$S \cdot \mathbf{n} = \mathbf{F}_A \quad (21)$$

where \mathbf{F}_A is the Gaussian pulse force applied to the ureter outer wall.

2.2.3 Fluid-Solid interaction ^{3,4}

The fluid and solid domains are coupled by using the arbitrary Lagrangian-Eulerian method (ALE). The total force that acts on the fluid-solid boundary due to the flow of urine is defined as:

$$f_r = \mathbf{n} \cdot [-p\mathbf{I} + \mathbf{K}] \quad (22)$$

Therefore, the force acting on the boundaries of the structure is

$$F_r = \boldsymbol{\sigma} \cdot \mathbf{n} \quad (23)$$

In order to couple these forces, there is a force transformation process performed using the ALE method.

$$F_r = f_r \cdot \frac{dv}{dV} \quad (24)$$

In Eq. (24), the mesh element factors are dv and dV for the fluid and material frames, respectively. Another coupling must be made to create a relation between the structural velocity of the moving solid wall and the fluid velocity

$$\mathbf{u}_{fluid} = \frac{\partial \mathbf{u}_{solid}}{\partial t} \quad (25)$$

2.3 Material Properties

2.3.1 Fluid

Urine is used as the fluid for the FSI simulation, and the urine is considered as Newtonian and incompressible fluid. The density of urine is 1050 kg/m^3 , with a dynamic viscosity of 1.3 cP .^[14-17] For the inlet and outlet boundary conditions of the ureter, an open boundary is considered^[14], making the flow exclusively driven by the peristaltic force on the outer wall of the ureter. The ureter wall is considered to have no-slip.

2.3.2 Solid

The ureter is considered as an isotropic, hyperelastic solid, based on the work of Rassoli.^[11] The default five-parameter Mooney-Rivlin model for hyperelastic materials was used to calculate the stress-strain relations of the material. High Mooney-Rivlin coefficients were used to give the ureter a highly elastic model, based on the work of Gomez-Blanco.^[6] The ureter is considered as a nearly incompressible material, with a bulk modulus κ of 1 GPa considerably higher than any of the Mooney-Rivlin coefficients. The ureteral density was taken as 1040 kg/m^3 .^[15]

For the ureteral stent, silicone was considered as a linear elastic, isotropic material. Silicone being obtained from COMSOL's material library, with E , ρ and ν being temperature dependent. A temperature of 310.15 K was chosen due to being the average body temperature. With this temperature input, E , ρ and ν were obtained. The stent was found to have a Young's Modulus of 4.22 MPa , Poisson ratio of 0.058 and density of 1261.1 kg/m^3 .

2.4 Setup of numerical simulation

The finite-element based numerical solver COMSOL Multiphysics was the software chosen for this work due to its capacity to couple different physics. The fluid-structure interaction was established as being fully coupled between the fluid and structural domain. The solid domain was solved using

Quadratic Lagrange discretization. A moving mesh was defined in the fluid domain with a Yeoh smoothing value of 10. A time-dependent study was performed for 3 seconds. A backward differentiation formula was used for time stepping. The initialization method used was Backward Euler. Initially, the fluid is at rest with inlet and outlet being open boundaries to obtain an initial solution, after the steady-state solution of fluid at rest is obtained, the peristaltic force begins being applied, turning it into a transient simulation. The PARDISO solver was used for both the fluid and mesh solutions and the MUMPS solver for the solid solutions.

2.4.1 Mesh

A 3D tetrahedral mesh was used for the simulation, with a finer mesh used in the fluid domain than in the solid domains. Hexahedral meshes were used in the fluid-solid boundaries for the boundary layer. 3 different meshes were tested in the Model No.3 of the ureter to validate mesh convergence. The average Von Mises stress across the stent length was compared between all meshes to study which mesh would provide the most accurate results, while saving computational expense. The meshes have 91261, 198071 and 499602 elements, respectively. The mesh independent study will be discussed in Section 3.

2.4.2 Boundary conditions

For the fluid simulation, the inlet and outlet boundaries were defined as open boundaries with no normal stress. The urine flow was defined as incompressible, Newtonian, laminar and the reference pressure was established as 130 Pa . The fluid walls were defined to have no slip.^[14]

For the solid domains, the top and bottom boundaries of both the ureter and the stent were defined to be fixed. The peristalsis mechanism was introduced as a Gaussian pulse being the boundary load acting on the outer surface of the ureter. The load was defined to travel in the positive direction of the coordinate frame to create an expansion of the ureter to develop the bolus of urine. The peristalsis mechanism was been modeled using a maximum load of $5 \times 10^4 \text{ N/m}^2$ with 1 cm of width traveling from inlet to outlet with a velocity of 2 cm/s .^[8] The force of the Gaussian pulse was chosen to create a 1 mm deformation perpendicular to the ureter wall.

3. RESULTS AND DISCUSSION

3.1 Mesh independent study

To test for the mesh convergence between the three meshes developed, the researchers used one of the stented models to develop a mesh refinement study. The parameter chosen to test for mesh convergence was the stent's average Von Mises stress as it varied with the ureter's length. The probe across the length was obtained creating a 3D line created in the middle of the ureteral stent, at about 0.75 mm from the center. The maximum stress difference between the 198071 and 499602 element meshes was not too considerable (as shown in Figure 3) taking into account the different in simulation times, so the 198071 element mesh was chosen to save computation times, while providing a good approximation of results.

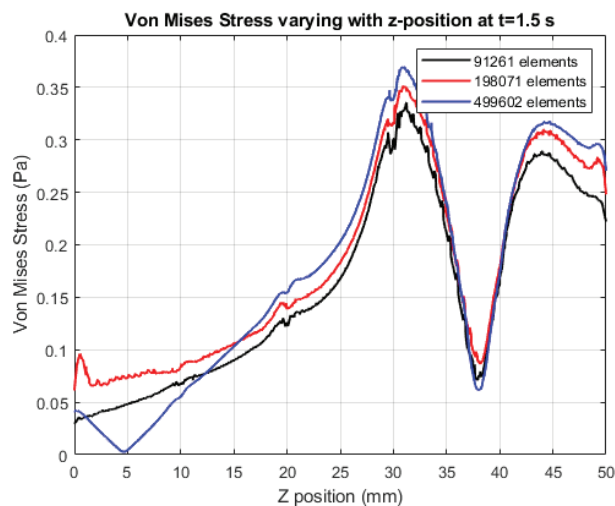


FIGURE 3: Mesh convergence study of the Von Mises stress at 1.5 s

3.2 The outlet flow rate

The outlet flow rate among various stents is important due to its validation of the stent's design. Medical professionals seek a stent that can help keep the urine flow as normal as if there was no stent present. A study of the outlet flow rate was performed using the z-velocity component from the flow simulation and taking the average velocity of the outlet surface. In Figure 4 we compared across the different 4 stent models in Table 1 and, while the results are similar for the most part, the model without stent experiences the least backflow. When the peristalsis is far from the outlet, all the outlet flow rates are negative, which indicate that the flow is trying to go back into the renal pelvis. However, when the peristaltic force reaches the outlet, the urine flows out as the flow rate increases and changes direction. This emulates the real mechanism of urine flow.

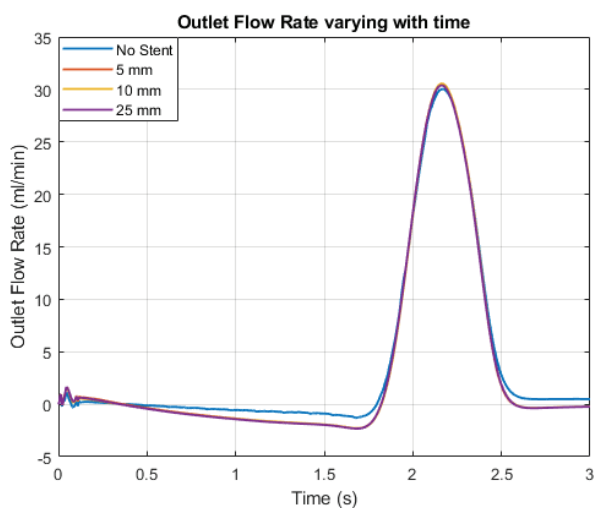
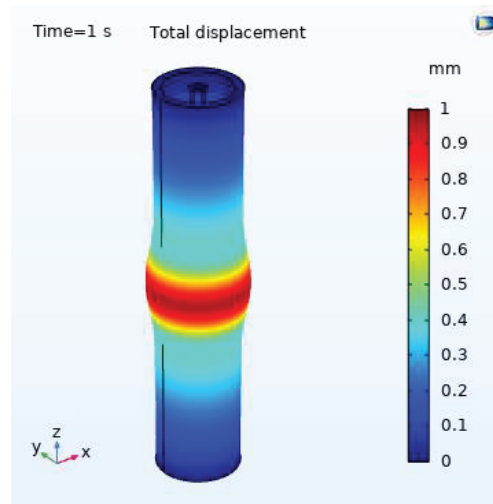
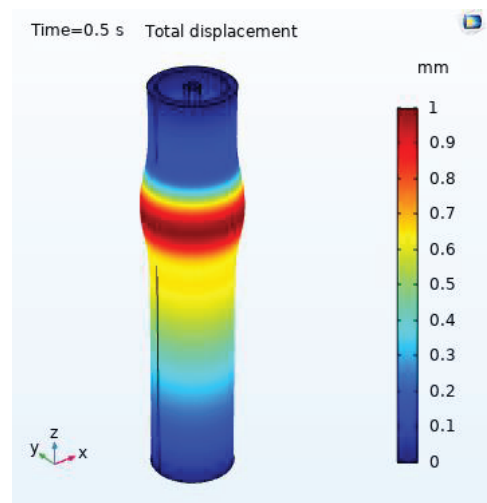


FIGURE 4: Outlet flow rate among different stent models

3.4 The displacement of ureter in the urine discharge process

The purpose of applying the ureteral stent is to allow for a proper discharge of urine. The difference in stent holes between the three stented models in Table 1 made it imperative to study the flow through the side holes themselves. The hole section located at the bottom of the model was studied at different time instants: 0.5, 1, 2 and 2.5 seconds. These times were chosen due to them being specifically when the peristalsis is at the top, middle, bottom of the model and far from the outlet, respectively. Figure 5 shows the location of the peristaltic wave across the length of the ureter at the different time instants. While the peristalsis is near the outlet, all the stented models have higher flow rates than the model without it.



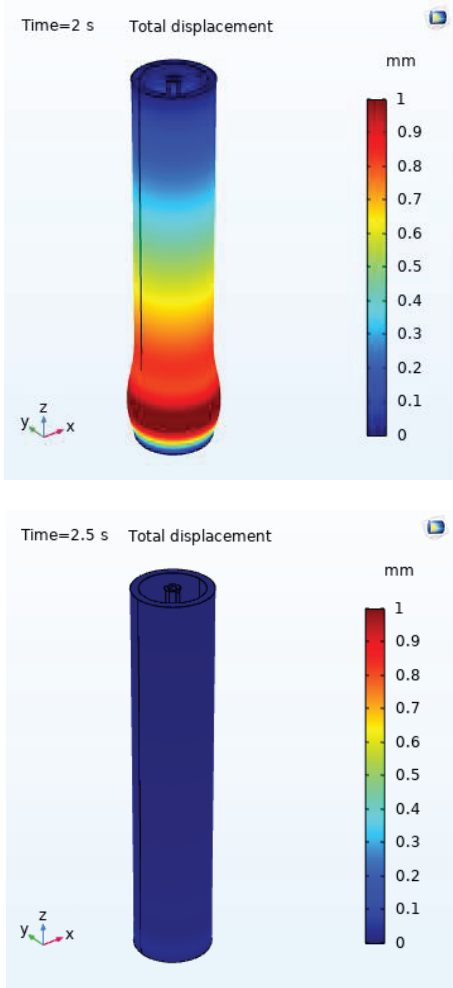


FIGURE 5: Peristaltic wave location at $t=0.5, 1, 2, 2.5$ s

3.5 The outlet stent-hole velocity in the urine discharge process

It is also important to explore the velocity at the stent-hole outlet, since higher velocity may also cause discomfort to the patients and eventually create very high stress for large displacement of the stent. From Figures 6-9, it can be inferred that the model with 5 mm distance between holes tends to show a lower y-velocity component as the distance from the center increases. The 25 mm distance model has a lower y-velocity closer to the center. The 10 mm distance having the higher velocity flowing through the side hole. It is also noticeable that when the peristaltic force reaches close to the studied discharge holes, the highest velocity through the hole is achieved.

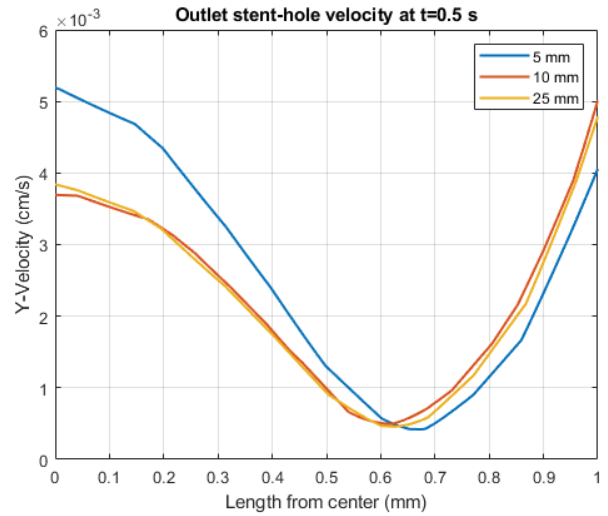


FIGURE 6: y-velocity through outlet stent hole at $t=0.5$ s

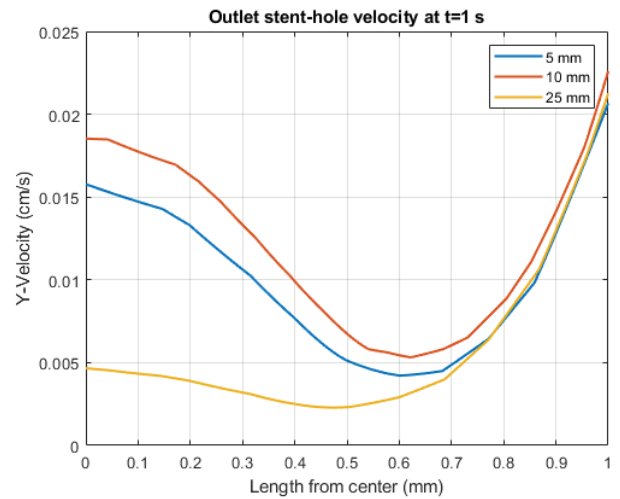


FIGURE 7: y-velocity through outlet stent hole at $t=1$ s

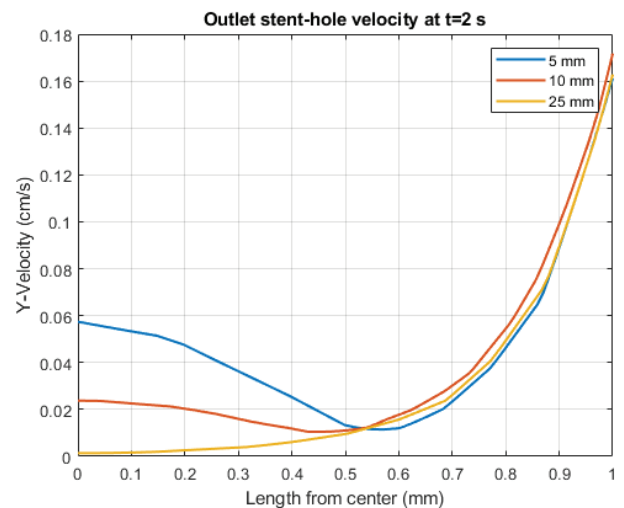


FIGURE 8: y-velocity through outlet stent hole at $t=2$ s

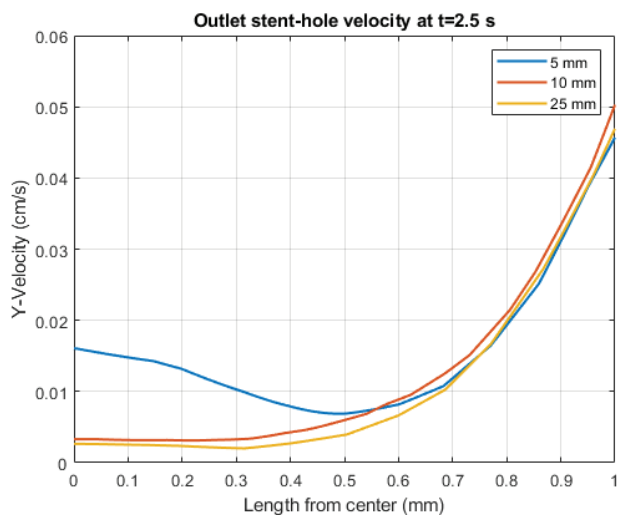


FIGURE 9: y-velocity through outlet stent hole at $t=2.5$ s

We can also observe from Figs. 6-9 that the y-velocity has a tendency to decrease first then increase, and this phenomenon matches well with the peristaltic wave shown in Fig. 5, therefore the peristaltic wave has a significant effect to the velocity distribution at the outlet of stent holes, eventually it will affect the stress distribution and the comfort feeling from the patients.

3.6 Maximum Von Mises stress in different stent models during the urine discharge process

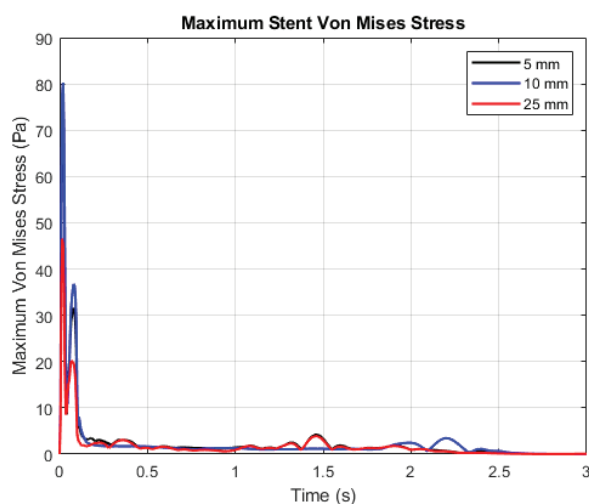


FIGURE 10: Maximum Von Mises stress in different stent models

Another important parameter in this study is the overall stress experienced by the stent with the peristaltic wave travelling across the ureter length. The physical meaning of the stent stress and its importance to urology is that the higher the stress encountered, the more displacement the stent will suffer, and subsequently, the higher the risk of the patient experiencing the discomfort and pain showcased by the stents' presence.

Additionally, as the stent is made out of silicone or other polymers, its stress can help prevent any fracture inside the body. Although the sole urine flow would be unable to go above the yield stress of the material, the movement of the human body can be an additional factor that can increase the stress encountered.

In this section, the three different stented models were compared through the maximum Von Mises stress experienced by the stent across time. The maximum stress is from the entire volume of the stent. From Figure 10 we can observe that the stent with 10 mm distance between side holes experienced the highest stress, with the 5 mm distance being close to it. The highest stresses the stent encounters seem to be at the beginning of the peristaltic expansion the ureter suffers. 10 mm seems to be an ideal distance between stent hole pairs in a perfectly straight ureter and stent. Although the 10 mm specimen suffers the highest Von Mises Stress values, the magnitude of the stress is not large enough for it to cause significant deformation on the stent. Nonetheless, further studies consisting in varying stent hole diameters and different positions of the stent resting in the ureter could help provide more evidence to this claim.

4. CONCLUSION

Ureteral stents are a measure used for many medical issues involving urology, such as kidney stones or kidney transplants. The purpose of applying stents is to help relieve the urine flow while the ureter is either blocked or trying to close itself, which creates blockages. In this study, we developed a fully coupled FSI model to explore how the ureter deforms due to peristalsis and the subsequent effect on the urine flow due to the ureter's deformation. Revising all the found results, the 10 mm stent model overall seems to provide the highest outlet flow rate, which indicates a proper stent design that allows for maximized urine discharge. This might point to the amount of side holes not being directly related to how much urine the stent can output. While the 10 mm model also suffers the highest stress out of all three stent models, the Von Mises stress is not high enough to deform the stent, whose yield strength is in the 10^6 Pa scale. This became the first study on the effect a peristaltic-driven urine flow has on the ureter stent, but more studies by varying stent hole diameters and different positions of the stent resting in the ureter are necessary to sustain this claim. We hope this study can help improve the stent design in kidney transplant procedures to further ease the inconvenience on the patients.

ACKNOWLEDGEMENTS

We want to acknowledge Dr. Phillip Thomas from the School of Medicine at University of Texas Rio Grande Valley for providing a clear introduction to urology and bringing light to the issue of ureteral stents to us. We need to appreciate the financial support from the Engaged Scholar Office at University of Texas Rio Grande Valley. The authors are also grateful for the support from the startup fund at Mississippi State University.

NOMENCLATURE

$C_{10}, C_{01}, C_{20}, C_{02}, C_{11}$ Mooney-Rivlin constants (Pa)
 E Young's Modulus of Elasticity (Pa)

ν	Poisson ratio
ρ	Density (kg/m^3)
μ	Fluid viscosity (cP)
\mathbf{u}_{fluid}	Velocity vector (m/s)
\mathbf{u}_{solid}	Displacement vector (m)
\mathbf{I}	Identity matrix
\mathbf{n}	Unit vector normal to surface
S	Second Piola-Kirchhoff Stress (Pa)
W_s	Strain energy density (J/m^3)
J	Jacobian
ϵ	Lagrangian Strain tensor
F	Deformation tensor
\mathbf{F}_v	Body forces (N)
\mathbf{F}_A	Gaussian pulse force (N/m^2)
\bar{I}_l	Strain invariant
C	Elasticity tensor
p	Pressure (Pa)

REFERENCES

- [1] Bevan, T., Carriveaul, R., Goneau, L., Cadieux, P., & Razvi, H. (2012). Numerical Simulation of Peristaltic Urine Flow in a Stented Ureter. *American Journal of Biomedical Sciences*, 233–248.
- [2] Boyarsky S, Labay PC. Ureteral dimensions and specifications for bioengineering modeling. In: Boyarsky P, Tanagho EA, Gottschalk CW, Zimskind PD, eds. *Urodynamics*. Academic Press; 1971:163-165.
- [3] COMSOL Multiphysics, “Structural Mechanics Module: User Guide”, Manual.
- [4] COMSOL Multiphysics, “CFD Module: User Guide”, Manual.
- [5] De Grazia, A., Somani, B. K., Soria, F., Carugo, D., & Mosayyebi, A. (2019). Latest advancements in ureteral stent technology. *Translational andrology and urology*, 8(Suppl 4), S436–S441. <https://doi.org/10.21037/tau.2019.08.16>
- [6] Gómez-Blanco, J. C., Martínez-Reina, F. J., Cruz, D., Pagador, J. B., Sánchez-Margallo, F. M., & Soria, F. (2016). Fluid Structural Analysis of Urine Flow in a Stented Ureter. *Computational and Mathematical Methods in Medicine*, 2016, 1–7.
- [7] J. H. Siggers et al., “Flow dynamics in a stented ureter” *Math Med Biol*, vol. 26, no. 1, pp. 1–24, 2009.
- [8] J. N. J. Lozano, *Peristaltic Flow with Application to Ureteral Biomechanics*, BiblioBazaar, Charleston, SC, USA, 2012.
- [9] L. J. Cummings et al., “The effect of ureteric stents on urine flow: Reflux,” *Journal of Mathematical Biology*, vol. 49, no. 1, pp. 56–82, 2004.
- [10] R. Venkatesh, J. Landman, S. D. Minor et al., “Impact of a double-pigtail stent on ureteral peristalsis in the porcine model: initial studies using a novel implantable magnetic sensor,” *Journal of Endourology*, vol. 19, no. 2, pp. 170–176, 2005.
- [11] Rassoli A, Shafigh M, Seddighi A, Seddighi A, Daneshparvar H, Fatourae N. Biaxial mechanical properties of human ureter under tension. *Urol J*. 2014 Jul 8;11(3):1678-86. PMID: 25015616.
- [12] Razavi, S. E., & Jouybar, M. (2018). Fluid-structure interaction simulation of ureter with vesicoureteral reflux and primary obstructed megaureter. *Bio-Medical Materials and Engineering*, 29(6), 821–837.
- [13] Sánchez, E. M., Blanco, J. C. G., Julia Estibaliz De La Cruz Conty, Margallo, F. M. S., Carrasco, J. B. P., & Gálvez, F. S. (2020). Simplified model of ureteral peristalsis bolus using fluid structure interaction. *Actas De Las XXXIX Jornadas De Automática*, Badajoz, September 5-7, 2018.
- [14] Takaddus, A. T., & Chandy, A. J. (2018). A three-dimensional (3D) two-way coupled fluid-structure interaction (FSI) study of peristaltic flow in obstructed ureters. *International Journal for Numerical Methods in Biomedical Engineering*, 34(10).
- [15] Takaddus, A. T., & Chandy, A. J. (2018). A two way fully coupled fluid structure simulation of human ureter peristalsis. *Computer Methods in Biomechanics and Biomedical Engineering*, 21(14), 750–759.
- [16] Takaddus, A. T., Gautam, P., & Chandy, A. J. (2016). Numerical Simulations of Peristalsis in Unobstructed Human Ureters. Volume 3: *Biomedical and Biotechnology Engineering*.
- [17] Takaddus, A. T., Gautam, P., & Chandy, A. J. (2018). A fluid-structure interaction (FSI)-based numerical investigation of peristalsis in an obstructed human ureter. *International Journal for Numerical Methods in Biomedical Engineering*, 34(9).
- [18] Vahidi, B., & Fatourae, N. (2007). A Numerical Simulation of Peristaltic motion in the Ureter Using Fluid Structure Interactions. 2007 29th Annual International Conference of the IEEE Engineering in Medicine and Biology Society.
- [19] Yang C, Bach RG, Zheng J, et al. In vivo IVUS-based 3-d fluid–structure interaction models with cyclic bending and anisotropic vessel properties for human atherosclerotic coronary plaque mechanical analysis. *IEEE Trans Biomed Eng*. 2009;56(10):2420-2428.
- [20] Yin F, Fung YC. Peristaltic waves in circular cylindrical tubes. *J Appl Mech*. 1969;36(3):579-587.